NONSTEADY MIXING WITH AN INCREASE IN HEAT-CARRIER FLOW RATE IN A BUNDLE OF COILED TUBES

B. V. Dzyubenko, L. A. Ashmantas, and A. B. Bagdonavichyus

UDC 621.564-71:536.423

A theoretical-experimental study is made of nonsteady mixing and generalizing relations are proposed for calculating the effective diffusion coefficient.

Heat exchangers with coiled tubes – in which heat transfer is intensified by swirling of the flow – are of great practical interest in areas of technology where it is necessary to not only reduce the weight and dimensions of the heat-exchanging equipment, but also to intensify interchannel mixing of the heat carrier [1]. Such equipment operates both under steady-state conditions and under conditions whereby the rate of flow of the heat carrier and the power of the thermal load change over time. These transients are characterized by high rates of change in the parameters and are of decisive importance in a number of cases. Thus, there is a need for theoretical-empirical study of nonsteady mixing of the heat carrier for different types of transience. Results of such studies were published in [2-6] for the cases of abrupt and smooth change in the power of the thermal load over time. The same investigations also examined different methods of experimentally studying and calculating nonsteady mixing of a heat carrier in a bundle of coiled tubes with an abrupt increase in the rate of flow of the heat carrier – leading to acceleration of the flow over time – and a thermal load of constant power.

To study nonsteady mixing under conditions of flow acceleration, we used the experimental unit described in [1], with some modifications. Specifically, we added (Fig. 1) a special device 17 to permit a sudden change in air flow rate, thus ensuring that the inertia of the system was low. The device altered the cross-sectional area of the tube, functioning similarly to an aperture stop in a camera. It was installed in front of a standard nozzle 7 provided to measure air flow rate (Fig. 1). The device works as follows. An electrical signal from the control system 18 travels through an amplifier to the electromagnetic valve of the air distributor 8, which is supplied with compressed air at a pressure of 0.6 MPa. From the distributor, the air travels to one of two chambers with spring-type energy accumulators, the exact chamber depending on the type of transience – associated with an increase or decrease in flow rate. The entry of the air into the chamber moves the chamber's rod, which with the aid of a lever transmits a rotating force to the lobes of the diaphragmlike device in the necessary direction. A special experiment was conducted to determine the inertia of the system for measuring time-varying air flow rate, which includes an SM-4 control computer. It was found that no more than 0.1 sec expires from the receipt of the signal (to activate the unit) by the SM-4 computer to recording of the measured quantity by the corresponding instrument.

An experimental study of nonsteady mixing was conducted by the method of heating the 37-tube central group of a bundle of coiled tubes with an electric current. The tubes, with an oval cross section, were electrically insulated from the unheated tubes in the bundle [1]. The entire bundle, consisting of 127 tubes, had a length of 0.5 m. The tubes, with a wall thickness of 0.2 mm, had a maximum oval dimension d = 12.3 mm and pitches S = 12d and S = 6.1d ($Fr_m = S^2/dd_e$) = 220 and 57). The temperature fields of the heat carrier were measured in the outlet section of the bundle with a group of 10 Chromel–alumel thermocouples. The diameter of the wire of the thermocouples was 0.1 mm. These sensors were installed on a coordinate-plotting mechanism at the centers of the cells at the points r/r_k = 0.073; 0.128; 0.193; 0.265; 0.334; 0.408; 0.479; 0.624; 0.770; 0.916. Air was used as the heat carrier.

Tests were conducted in the ranges Fr_m = 57-220, heat-load power N = 5.166-8.6 kW, ratio of the maximum heat-carrier flow rate after perturbation G_2 to its initial stead-state value

Translated from Inzhenerno-Fizicheskii Zhurnal, Vol. 55, No. 3, pp. 357-363, September, 1988. Original article submitted May 18, 1987.

0022-0841/88/5503-0947$12.50

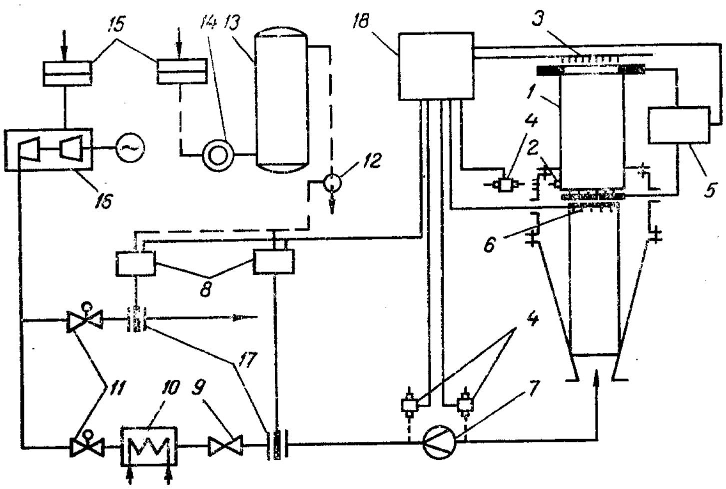

Fig. 1. Basic diagram of the experimental unit: 1) test section; 2) pressure release; 3) coordinate-plotting mechanism with thermocouples; 4) pressure gauges; 5) dc generator; 6) thermocouples at bundle inlet; 7) nozzle to measure flow rate; 8) main pneumatic drive; 9) valve; 10) condenser; 11) automatic valves; 12) reducer; 13) receiver; 14) compressor; 15) filter; 16) turbocompressor; 17) device for measuring flow rate; 18) automatic measurement and control system.

G_1 G_2/G_1 = 1.12-1.77, numbers $Re_2 = 7.1 \cdot 10^3 - 1.2 \cdot 10^4$, maximum value of the parameter K_G = $(0.0478-2.46) \cdot 10^3$. The regime parameters realized in the tests are shown in Table 1 and Fig. 2. It can be seen from Fig. 2 that the highest value of the new flow rate G_2 was reached after the period τ = 0.4-0.8 sec, reckoned from the introduction of the perturbation. Flow rate then decreased somewhat and reached a new steady-state value greater than G_1 after another 3-4 sec. Here, since the thermal load remained unchanged during the experiment, the mean mass temperature of the flow at the bundle outlet decreased. In accordance with this, there was also a reduction in the temperature of the wall of the coiled tubes.

The main goal of the experiment was to determine relations for calculating effective nonsteady diffusion coefficients with flow acceleration and N = const.

In determining the effective diffusion coefficient $K = D_t/ud_e$ of the type of transience being examined here, we compared experimental and theoretical temperature fields of a heat carrier reported in [1-6]. With a sharp increase in flow rate, the temperature fields were calculated in accordance with [2-6] by numerically solving a system of differential equations describing the flow of a homogenized medium. Here, the gasdynamic equations were written in a quasi-stationary approximation, with use of the experimental dependence of heat-carrier flow rate on time $G = G(\tau)$ (Fig. 2). The initial conditions of the problem were determined from calculation of the steady-state regime existing before perturbation of the system (with G_1 = const and N = const).

Figure 3 shows typical experimental temperature fields of the heat carrier (in the form of individual points) in a bundle of coiled tubes with Fr_m = 57 for different moments of time. This data is compared with theoretical temperature curves for different values of the coefficient K_n. It is apparent that at the initial moment of time (τ = 0), the coefficient K is equal to the quasistationary value K_{qs} = 0.09. After the introduction of a perturbation into the flow through an increase in flow rate G_2/G_1 = 1.77, the coefficient K_n at first decreases sharply (by a factor of 2-2.5) relative to K_{qs}. It then increases smoothly and, at $\tau \approx 10$ sec, becomes equal to the quasi-stationary value.

This pattern of change in the coefficient $K_n = f(\tau)$ is connected with the fact that the thermal inertia of the tubes exerts the dominant effect on K_n in the case being examined. Here, the change in the temperature fields of the heat carrier over time is similar in character to the change in the temperature fields seen with a decrease in the thermal load over time [5, 6]. This result is not unexpected. In fact, with an increase in the flow rate of the heat carreir and a constant thermal load on the coiled tubes, the temperatures of the tube walls and heat carrier decrease. The latter should in turn lead to a reduction in the coefficient K_n or in the relative coefficient $\varkappa = K_n/K_{qs}$, since additional heat is

TABLE 1. Regime Parameters Realized in Experiments with Acceleration of the flow

№	G_2/G_1	Fr_m	N, kW	$K_G \cdot 10^{-3}$	G_2, kg/sec	$\left(\frac{\partial G}{\partial \tau}\right)_m$, kg/sec^{-2}
1	1,77	220	5,958	1,45	0,2894	0,315
2	1,73	220	5,166	0,7	0,2456	0,129
3	1,71	220	5,915	2,46	0,2835	0,52
4	1,68	220	7,17	2,29	0,3365	0,582
5	1,77	57	6.4	1,42	0,2640	0,288
6	1,62	57	7,5	0,465	0,2666	0,1022
7	1,12	57	8,6	0,0478	0,242	0,0135

released into the flow as the wall cools when the thermal load is kept constant. At the same time, it is known that in the heating of a gas with T_w = const in circular tubes, flow acceleration increases the parameter $K_\alpha = Nu_n/Nu_{qs}$ [7]. The superposition of the effects of these two mechanisms on nonsteady heat transfer can evidently explain the constancy of the coefficient $K_n = K_{qs}$ over time within the range of variation of the flow-rate ratio $1.12 > G_2/G_1 > 1$. Since a change in flow rate $\partial G/\partial\tau$ at N = const is accompanied by a change in the cooling of the walls of the coiled tubes and manifestation of the temperature derivatives $\partial T_w/\partial\tau$ and $\partial T_b/\partial\tau$, in accordance with [6], the process of nonsteady mixing of a heat carrier in a bundle of coiled tubes must be influenced by a parameter of the form

$$K_{Tg}^{*'} = \frac{\partial T_b}{\partial \tau}\frac{1}{T_b}\sqrt{\frac{\lambda_b}{ug\rho_b c_p}}, \tag{1}$$

$$K_G = \frac{\partial G}{\partial \tau}\frac{d_k^2}{G\nu_b}. \tag{2}$$

The parameter $K^{*'}_{Tg}$ considers the effect of the nonsteady change in flow temperature on thermal resistance between the wall and the flow in a bundle cell and between cells. The parameter K_G characterizes the effect of the change in the rate of flow of the heat carried on the nonsteady mixing process. However, introduction of the parameter $K^{*'}_{Tg}$ in [2] did not enable the authors to satisfactorily generalize empirical data on the coefficient $\varkappa$ with a sharp increase in the thermal load. The greatest scuccess in [2-6] was attained when empirical data corresponding to a change in the thermal load was generalized by using the Fourier criterion

$$Fo_b = \frac{\lambda_b \tau}{c_p \rho_b d_k^2}. \tag{3}$$

In the case of an increase in the flow rate of the heat carrier (acceleration of the flow) with a constant thermal load, the criterion K_G (2) also fails to allow derivation of a relation $\varkappa = f(K_G)$ which generalizes empirical data (see Tables 1 and 2). Thus, it is best to also use the criterion Fo_b and the parameter G_2/G_1 – respectively characterizing the restructuring of the temperature fields in the flow core and acceleration of the flow at N = const – as the main criteria of similitude in the given case. Thus, we then seek a criterional relation of the form

$$\varkappa = f(Fo_b, G_2/G_1, Fr_m). \tag{4}$$

Figure 4 shows our experimental data (Table 2) in the form of the dependence of the coefficient $\varkappa$ on the Fourier criterion Fo_b for different values of the flow-rate ratio G_2/G_1 and different numbers Fr_m. It is evident that $\varkappa$ decreases sharply just after flow rate is increased. It then smoothly approaches unity ($K_n = K_{qs}$). The family of curves shown in Fig. 4 can be described by the functional relation

$$\varkappa = A\,Fo_b^n + C, \tag{5}$$

where the quantities A, n, and C have the following values for different numbers Fr_m and G_2/G_1: for $Fr_m = 57$, $G_2/G_1 = 1.62$: A = 3.89; n = 0.0764, C = −1.66; for $Fr_m = 220$, $G_2/G_1 = 1.68$: A = 3.846, n = 0.0966, C = −1.425; for $Fr_m = 220$, $G_2/G_1 = 1.71$: A = 3.758, n = 0.240, C = −0.210; for $Fr_m = 220$, $G_2/G_1 = 1.73$: A = 3.758, n = 0.240, C = − 0.235; for $Fr_m = 57$; 220, $G_2/G_1 = 1.77$: A = 3.758 n = 0.2476, C = −0.221. Equation (5) is valid at $Fo_b > 8\cdot10^{-3}$ and $\varkappa \leqq 1$.

For $G_2/G_1 = 1.77$, the test data on the coefficient $\varkappa$ for bundles of coiled tubes with Fr_m = 57 and 220 is described by a single curve (Fig. 4). Thus, the number Fr_m for the given

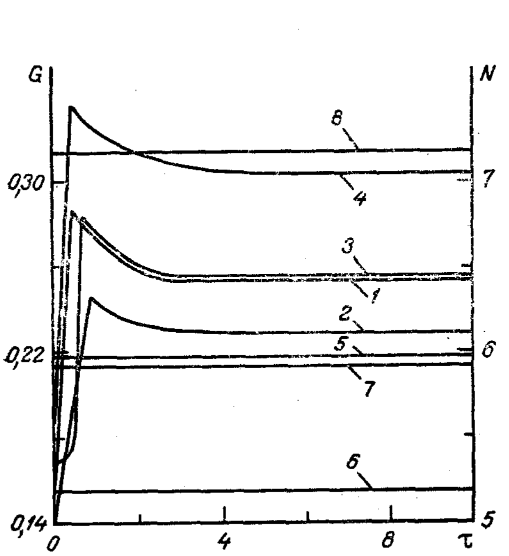

Fig. 2

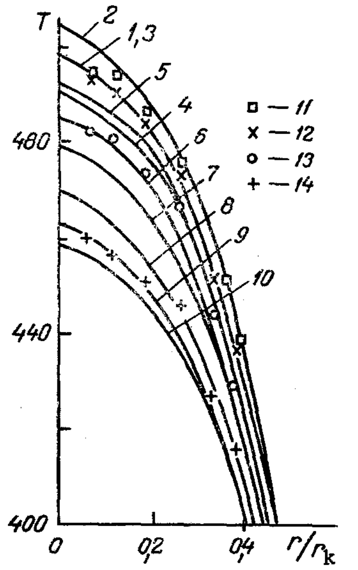

Fig. 3

Fig. 2. Change in heat-carrier flow rate (1-4) and the thermal load (5-8) over time for the case of flow acceleration in a bundle with $Fr_m = 220$ at $G_2/G_1 = 1.77$; 1.73; 1.71; 1.68, respectively. G, kg/sec; N, kW; τ, sec.

Fig. 3. Temperature field of the heat carrier in the outlet section of a bundle with $Fr_m = 57$ at $N = 6.4$ kW and $G_2/G_1 = 1.77$: curves show theoretical temperature fields at $\tau = 0$ and $K = 0.09$ (1); 0.8 and 0.03 (2); 0.8 and 0.05 (3); 0.8 and 0.07 (4); 2.8 and 0.05 (5); 2.8 and 0.07 (6); 2.8 and 0.09 (7); 10 and 0.07 (8); 10 and 0.09 (9); 10 and 0.1 (10); points show experimental data for $\tau = 0$ (11), 0.8 (12), 2.8 (13), 10 sec (14). T, K.

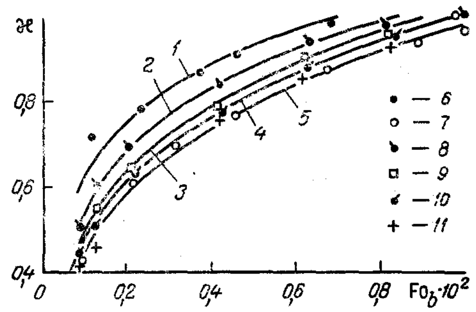

Fig. 4. Dependence of the relative mixing coefficient $\varkappa$ on the Fourier number with different values of Fr_m and different flow-rate ratios G_2/G_1: 1-5) Exp. (5) with $G_2/G_1 = 1.62$; 1.68; 1.71; 1.73; 1.77; respectively; 6, 7) experimental data for $Fr_m = 57$ at $G_2/G_1 = 1.62$ and 1.77; 8-11) same for $Fr_m = 220$ at $G_2/G_1 = 1.68$; 1.71; 1.73; 1.77.

type of transience has almost no effect on the relative mixing coefficient $\varkappa = K_n/K_{qs}$ within the range $Fr_m = 57$-220. The number Fr_m has no effect on the coefficient $\varkappa$ either with a sharp increase in the rate of flow of the heat carrier (acceleration of the flow) or with a reduction in the power of the thermal load, i.e., in those cases when the character of change in the nonsteady characteristics of the temperature fields of the heat carrier over time is the same. This shows that the process of nonsteady heat transfer is controlled mainly by restructuring of the temperature fields connected with the effect of nonsteady boundary conditions. Thus, for the type of transience being examined, instead of using criterional relation (4), we use the following expression to determine the coefficient $\varkappa$

$$\varkappa = f(Fo_b,\ G_2/G_1). \tag{6}$$

TABLE 2. Change in the Coefficients K_n and $\varkappa$ over Time with Acceleration of the Flow

No. of regime (Table 1)	Param-eter	Time τ, sec											
		0	0,8	1	1,2	2	2,8	3	4	6	7,8	8	10
1	K	0,07	0,029	—	0,032	0,043	—	—	0,053	0,06	—	0,064	—
	$\varkappa$	1	0,415	—	0,456	0,615	—	—	0,756	0,857	—	0,915	—
2	K_n	0,07	0,03	—	0,035	0,0447	—	—	0,0542	0,061	—	0,066	—
	$\varkappa$	1	0,429	—	0,5	0,637	—	—	0,775	0,87	—	0,942	—
3	K_n	0,07	—	—	0,038	0,045	—	—	0,055	0,063	—	0,067	0,07
	$\varkappa$	1	—	—	0,542	0,643	—	—	0,786	0,90	—	0,956	1
4	K_n	0,07	0,035	—	0,042	0,049	—	—	0,058	0,066	0,068	—	0,07
	$\varkappa$	1	0,5	—	0,6	0,7	—	—	0,828	0,942	0,97	—	1
5	K_n	0,09	0,038	—	—	0,057	0,063	—	0,069	0,0785	—	0,084	0,0865
	$\varkappa$	1	0,422	—	—	0,634	0,7	—	0,767	0,875	—	0,935	0,96
6	K_n	0,09	—	0,065	—	0,071	—	0,078	0,082	0,088	—	—	0,09
	$\varkappa$	1	—	0,722	—	0,79	—	0,868	0,91	0,979	—	—	1
7	K_n	0,09	—	—	—	0,09	—	—	—	0,09	—	—	0,09
	$\varkappa$	1	—	—	—	1	—	—	—	1	—	—	1

It is evident from Fig. 4 that an increase in the ratio G_2/G_1 is accompanied by an increase in the difference between the nonstationary coefficient K_n and its quasistationary value K_{qs}. The character of the dependence of the coefficient $\varkappa$ on the ratio G_2/G_1 can be illustrated for the number $Fo_b = 10^{-3}$ by the expression

$$\varkappa = -0,85(G_2/G_1)^2 + 1,62(G_2/G_1) + 0,27. \tag{7}$$

For other values of the number Fo_b, the numerical values of the coefficients entering into (7) will change accordingly.

Thus, the relations found for calculation of the coefficient $\varkappa$ make it possible to close the system of differential equations which describes nonsteady heat transfer in bundles of coiled tubes [2-6] and to calculate the thermohydraulic parameters of heat exchangers with the above-examined type of transience. The laws established for nonsteady mixing with flow acceleration show that there is a reduction in the effective diffusion coefficient K_n during the initial moments of time compared to its quasistationary value. However, since an increase in the rate of flow of the heat carrier is accompanied by a marked reduction in the mean mass temperature of the carrier, the effect of the reduction in K_n relative to K_{qs} under conditions of nonuniform heat delivery over the radius of the bundle may be insignificant from the viewpoint of the performance of the heat exchanger.

NOTATION

N, power of the thermal load; τ, time; G_1, initial flow rate of heat carrier; G_2, maximum flow rate of heat carrier after introduction of perturbation into the supply system; K, dimensionless effective diffusion coefficient; D_t, effective diffusion coefficient; u, velocity; d_e, equivalent diameter of the bundle; Fr_m, coefficient characterizing features of the flow in a bundle of coiled tubes; S, pitch of tube; d, maximum dimension of tube profile; Fo, Fourier criterion; a, diffusivity; d_k, r_k, diameter and radius of tube bundle; λ_b, thermal conductivity; c_p, heat capacity; ρ_b, density; Re, Reynolds number; ν, kinematic viscosity; $\varkappa$, relative diffusion coefficient; T, temperature; r, radial coordinate; K_G, parameter accounting for the effect of nonsteady flow rate; Nu, Nusselt number. Indices: b, mean-mass; w, wall; n, nonstationary; qs, quasistationary.

LITERATURE CITED

1. Yu. I. Danilov, B. V. Dzyubenko, G. A. Dreitser, L. A. Ashmantas, Heat Exchange and Hydrodynamics in Channels of Complex Form [in Russian], Moscow (1986).
2. B. V. Dzyubenko, M. D. Segal', L. A. Ashmantas, and P. A. Urbonas, Izv. Akad. Nauk SSSR, Énerg. Transp., No. 3, 125-133 (1983).
3. B. V. Dzyubenko, L. A. Ashmantas, M. D. Segal', and P. A. Urbonas, Izv. Akad. Nauk SSSR, Énerg. Transp., No. 4, 110-118 (1985).
4. B. V. Dzyubenko, L. A. Ashmantas, and A. B. Bagdonavichyus, Current Problems of Hydrodynamics and Heat Transfer in Elements of Power Plants and Cryogenic Technology: Interinstitute Collection of Scientific Transactions, Vol. 14, Moscow (1985), pp. 9-14.

5. B. V. Dzyubenko, L. A. Ashmantas, A. B. Bagdonavichyus, and M. D. Segal', Inzh.-Fiz. Zh., 54, No. 4, 533-539 (1988).
6. L. A. Ashmantas, B. V. Dzyubenko, G. A. Dreitser, and M. D. Segal, Int. J. Heat Mass Transfer, 28, No. 4, 867-877 (1985).
7. É. K. Kalinin, G. A. Dreitser, V. V. Kostyuk, and I. I. Berlin, Methods of Calculating Coupled Heat-Transfer Problems [in Russian], Moscow (1983).

STUDY OF A FINNED TWO-CHAMBER VORTEX TUBE

A. N. Azarov and P. E. Krotov UDC 621.565.3

A two-chamber "module" of a multichamber vortex-type cold-air machine is examined in four operating regimes.

Vortex tubes with internal and external finning of the cold-cooled energy-separating chamber [1, 2] are used in small air-conditioning units for commercial electronics, in devices providing individual and group protection of workers from heat in hot shops, and in other applications. Expansion of the range of use of this equipment is requiring a further improvement in their service characteristics. The foremost needs are to increase the range of temperature control and the discharge of cooled flow and to enable the equipment to be attached to existing air supply system – which are chracterized by a wide range of compressed-air pressures. The use of two-chamber [3] and multichamber [4] vortex units has some potential in this regard.

The simplest two-chamber module of a multichamber vortex-type cold-air machine is a design with identical ($\overline{F}_1 = \overline{F}_2$; regime A) or different ($\overline{F} \neq \overline{F}_2$; regime B) inlet sections in the swirl chambers (Fig. 1). If necessary, only one inlet ($\overline{F}_1$ or $\overline{F}_2$; regime C) can be connected to a compressed-air main. It is also interesting to explore the possibility of producing cold with two inlet connected to the source ($\overline{F}_1$ and $\overline{F}_2$) but with the removal of the cold flow through a single outlet channel 3 (regime D) rather than two, as in regimes A, B, and C.

Figure 2 schematically depicts the operating regimes of the two-chamber module.

The diameter of the swirl chambers of the module we studied was 38 mm; the relative cross-sectional area of the inlets $\overline{F}$ = 0.08-0.11, the length of the unfinned initial section 7 (see Fig. 1) was 114 mm, the distance between the nozzle sections of inlets 1 and 2 (the axial length of the module without the outlet channels 3) was 533 mm, and the area of the internal and external finning was 0.21 and 2.94 m^2, respectively.

Tests were conducted with undried compressed air. The temperature in the experiment was measured by thermocouples to within 0.1 K, pressure was measured by manometers with an accuracy of class 0.6, and flow rates were determined by means of Venturi meters.

In regime A, we obtained two cold flows with identical temperatures and flow rates. Figure 3a shows the temperature-energy characteristics of a two-chamber module with cold-flow outlet channels in the form of a pipe (solid curves) or a slitted diffuser (dashed lines).

In regime B, the discharge of the cold flows was redistributed in the following proportion

$$\frac{G_{x1}}{G_{x2}} = \frac{F_1}{F_2}. \tag{1}$$

Thus, a swirl chamber with a large inlet cross section operates at $\mu_1 = G_x/G_c < 1$, while the second chamber studied operates at $\mu_2 > 1$. The temperatures of the cold flows in the left and right outlet channels 3 (see Fig. 1) were different, with the size of the axial hole 6 in the central fin having a decided effect on this difference. The relative diameter of

Odessa Engineering Institute of the Refrigeration Industry. Translated from Inzhenerno-Fizicheskii Zhurnal, Vol. 55, No. 3, pp. 363-366, September, 1988. Original article submitted April 27, 1987.

 0022-0841/88/5503-0952$12.50